

Balance of unidirectional monovalent ion fluxes in cells undergoing apoptosis: why does Na⁺/K⁺ pump suppression not cause cell swelling?

Valentina E. Yurinskaya, Andrey A. Rubashkin and Alexey A. Vereninov

Laboratory of Cell Physiology, Institute of Cytology, Russian Academy of Sciences, Tikhoretskii prospect 4, 194064 Saint Petersburg, Russia

Non-technical summary Apoptosis is a crucial mechanism for tissue maintenance and deregulation of apoptosis may lead to catastrophic consequences in humans (e.g. cancer). The present work is a first attempt to quantitatively characterize rearrangement of the monovalent ion fluxes in cells during apoptosis. An established model of apoptosis induced by staurosporine in lymphoid U937 cells is used to experimentally measure cellular Cl⁻ content and fluxes, K⁺, Na⁺ and water content as well as ouabain-sensitive and -resistant Rb⁺ fluxes. A mathematical model is developed to account for the unidirectional ion fluxes and water balance in a cell as a whole. A decrease in the channel permeability of the plasma membrane for Na⁺ proved to be crucial for preventing cell swelling due to the decrease in Na⁺/K⁺ pump activity in cells undergoing apoptosis whereas opening of the K⁺ and Cl⁻ channels is not required. Supplemental Table S1 is given for easy calculating flux balance under specified conditions.

Abstract Cells dying according to the apoptotic program, unlike cells dying via an unprogrammed mode, are able to avoid swelling and osmotic bursting with membrane disruption. There are indications that apoptosis is accompanied by suppression of the Na⁺/K⁺ pump and changes in the K⁺ and Cl⁻ channels. It remains unclear how ion fluxes through individual ion pathways are integrated so as to induce loss of intracellular ions and concomitant apoptotic volume decrease. A decrease in activity of the sodium pump during apoptosis should cause cell swelling rather than shrinkage. We have made the first systemic analysis of the monovalent ion flux balance in apoptotic cells. Experimental data were obtained for human U937 cells treated with staurosporine for 4–5 h, which is known to induce apoptosis. The data include cellular Cl⁻ content and fluxes, K⁺, Na⁺, water content and ouabain-sensitive and -resistant Rb⁺ fluxes. Unidirectional monovalent ion fluxes were calculated using these data and a cell model comprising the double Donnan system with the Na⁺/K⁺ pump, Cl⁻, K⁺, Na⁺ channels, the Na⁺-K⁺-2Cl⁻ cotransporter (NKCC), the Na⁺-Cl⁻ cotransporter (NC), and the equivalent Cl⁻/Cl⁻ exchange. Apoptotic cell shrinkage was found to be caused, depending on conditions, either by an increase in the integral channel permeability of membrane for K⁺ or by suppression of the pump coupled with a decrease in the integral channel permeability of membrane for Na⁺. The decrease in the channel permeability of membrane for Na⁺ plays a crucial role in cell dehydration in apoptosis accompanied by suppression of the pump. Supplemental Table S1 is given for easy calculating flux balance under specified conditions.

(Resubmitted 17 February 2011; accepted 4 March 2011; first published online 21 March 2011)

Corresponding author A. A. Vereninov: Laboratory of Cell Physiology, Institute of Cytology, Russian Academy of Sciences, Tikhoretskii prospect 4, 194064 Saint-Petersburg, Russia. Email: verenino@mail.ru; verenino@gmail.com

Abbreviations AVD, apoptotic volume decrease; KCC, K⁺-Cl⁻ cotransporter; NC, Na⁺-Cl⁻ cotransporter; NKCC, Na⁺-K⁺-2Cl⁻ cotransporter; NMDG, N-methyl-D-glucamine; NPPB, 5-nitro-2-(3-phenylpropylamino) benzoic acid; RVD, regulatory volume decrease; RVI, regulatory volume increase; STS, staurosporine.

Introduction

Cells dying according to the apoptotic program, unlike cells dying via an unprogrammed mode, are able to prevent swelling and osmotic bursting with membrane disruption. Intracellular macromolecular compounds can exit into the interstitial medium therefore only after enzymatic splitting or in 'containers' such as 'apoptotic bodies'. Apoptosis has been defined historically as a 'shrinkage necrosis' (Kerr, 1971). There is abundant evidence that ion channels and transporters are involved in apoptosis (Burg *et al.* 2006; Lang *et al.* 2006, 2007, 2008; Okada *et al.* 2006; Bortner & Cidlowski, 2007). An important function of the ion transporting system is maintenance of the cell water balance (Hoffmann *et al.* 2009). A decrease in activity of the sodium pump, and an increase in opening of the K^+ and Cl^- channels, are believed to be responsible for the loss of intracellular ions and concomitant apoptotic cell shrinkage (Nobel *et al.* 2000; Bortner *et al.* 2001). The extent to which changes in ion fluxes through distinct ion pathways are integrated so as to give rise to cell shrinkage specific to apoptosis is not settled, however. In particular, the decrease in the sodium pump activity during apoptosis should lead to cell swelling, but in fact shrinkage occurs (Maeno *et al.* 2000, 2006; Okada & Maeno, 2001). Opening of the K^+ channels should be associated with cell hyperpolarization, but depolarization has been reported (Franco *et al.* 2006). We have studied the total monovalent ion flux balance in apoptotic cells. A body of experimental data was obtained for an established model of apoptosis, namely human lymphoid cells U937 treated with staurosporine (STS). The data include the intracellular Cl^- content and fluxes, K^+ , Na^+ content, ouabain-sensitive and -resistant Rb^+ fluxes and cell water content. These data are mathematically sufficient to calculate the total monovalent flux balance in a cell model with the Na^+/K^+ pump, Cl^- , K^+ and Na^+ channels, and NKCC and NC cotransport, i.e. with all major players in maintenance of the monovalent ion and water balance in animal cells (Hoffmann *et al.* 2009).

Modelling of the total monovalent ion flux balance during apoptosis yielded some new and unexpected results. A decrease in the integral channel permeability of membrane for Na^+ appeared to be crucial in preventing the cell swelling which should be caused by a decrease of pump activity in cells undergoing apoptosis. The model showed that apoptotic cell shrinkage can occur without an increase in opening of the K^+ channels. Characterizing the specific role of monovalent ions in cell water regulation during apoptosis is a principal aim of this study. The work also provides a computational model for analysis of ion fluxes and water balance in cells.

Methods

Reagents

RPMI 1640 medium and fetal bovine serum (FBS, HyClone Standard) were purchased from Biotot (Russia). Staurosporine (STS), ouabain, bumetanide, 4,4-diisothiocyanatostilbene-2,2-disulfonic acid (DIDS), 5-nitro-2-(3-phenylpropylamino)benzoic acid (NPPB), *N*-methyl-D-glucamine (NMDG) and glutamic acid were purchased from Sigma-Aldrich (Germany). Percoll was from Pharmacia (Sweden). The isotope $^{36}Cl^-$ was from 'Isotope' (Russia). Salts were of analytical grade and were from Reachem (Russia).

Cell cultures

Three strains of U937 cells were studied: cells of strains 1 and 2 (Cells 1 and 2) were obtained from the Russian cell culture collection (Institute of Cytology, Russian Academy of Sciences, catalogue numbers U937-160B2 and U937-9957, respectively). Cells of strain 3 were obtained from the German Collection of Microorganisms and Cell Cultures (DSMZ). Cells 1a and 1b denote independent series of experiments. Cells were cultured in RPMI 1640 medium supplemented with 10% FBS at 37°C and 5% CO_2 . For induction of apoptosis, the cells, at a density of 1×10^6 cells ml^{-1} , were exposed to staurosporine for 4–5 h. All the incubations were done at 37°C.

Determination of intracellular ion content and Rb^+ influx

Intracellular K^+ , Na^+ and Rb^+ content was measured by emission photometry in an air–propane flame using a Perkin-Elmer AA 306 spectrophotometer, as described previously (Yurinskaya *et al.* 2005a,b). In summary, the cells were pelleted in RPMI medium, washed five times with $MgCl_2$ solution (96 mM) and treated with 5% trichloroacetic acid (TCA). TCA extracts were analysed for ion content. To study Rb^+ influx, a 50 mM stock solution of $RbCl$ was added to 1 ml of cell suspension ($\sim 1 \times 10^6$ cells) so as to yield 2.5 mM final concentration of Rb^+ . Cells were incubated with Rb^+ for 10 min at 37°C with or without 0.1 mM ouabain. It has been shown previously for U937 cells that Rb^+ is a good substitute for K^+ , as in many other cells, and that ouabain-sensitive Rb^+ influx should be measured for short time intervals (5–10 min), since treatment of cells with ouabain for more than 10 min was followed by a remarkable increase in cell Na^+ content (Vereninov *et al.* 2007). To determine the intracellular Cl^- , cells were cultured for 90 min or more at 37°C in RPMI medium containing $^{36}Cl^-$ ($0.12 \mu Ci ml^{-1}$, Isotope,

Russia). The radioactivity of ³⁶Cl⁻ in TCA extracts was measured using a liquid scintillation counter (Beckman LS 6500).

The intracellular Cl⁻ content was calculated taking into account the specific activity of ³⁶Cl⁻ (~2 counts min⁻¹ μmol⁻¹). The TCA precipitates were dissolved in 0.1 N NaOH and analysed for protein by the Lowry procedure, with serum bovine albumin as a standard. The cell ion content was calculated in micro-moles per gram of protein.

Determination of cell water content

Cell water was determined by measurements of the buoyant density of the cells in a continuous Percoll gradient, as described previously (Yurinskaya *et al.* 2005a,b; Vereninov *et al.* 2008). In summary, the Percoll solution was prepared according to the manufacturer's instruction and a thick cell suspension (0.1–0.2 ml, ~3 × 10⁶ cells) was placed on the solution surface and centrifuged for 10 min at 400 g (MPW-340 centrifuge, Poland). The buoyant density of the cells was estimated using density marker beads (Sigma-Aldrich, Germany). The water content per gram of protein, v_{prot} , was calculated as $v_{\text{prot}} = (1 - \rho/\rho_{\text{dry}})/(0.79(\rho - 1))$, where ρ is the measured buoyant density of the cells and ρ_{dry} is the cell dry mass density, which was 1.35 g ml⁻¹. The proportion of protein in dry mass was 79%. The relative changes in cell water are virtually independent of the values of ρ_{dry} and the protein proportion, whereas the absolute water content does exhibit dependence on these values.

Study of ³⁶Cl⁻ gain and release from cells; calculation of fluxes and rate constants

To study the time course of ³⁶Cl⁻ uptake, the cells were cultured in RPMI medium with ³⁶Cl⁻ (0.12 μCi ml⁻¹) for 5 min, 10 min and 90 min at 37°C. The samples containing cells were then prepared as for the ion content assay (Yurinskaya *et al.* 2010). To determine the rate of ³⁶Cl⁻ release, the cells were preloaded with the tracer for 90 min at 37°C. Then cells were sedimented by centrifuging, washed with 96 mM MgCl₂ solution and resuspended in ³⁶Cl⁻-free RPMI medium for 5 or 10 min at 37°C so as to attain a final concentration of (1–2) × 10⁶ cells ml⁻¹. The cells and the incubation medium were then analysed for ³⁶Cl⁻ content. The ion tracer exchange between the cell and the medium was fitted by equations: $y(t) = y_{\infty}(1 - \exp(-kt))$ for the ion gain and $y(t) = y_0 \exp(-kt)$ for ion release where $y(t)$ is the tracer content at time t and y_{∞} and y_0 are the final and initial contents; here k is the rate constant of ion equilibration, the same in both equations. This rate constant k was calculated from these equations for the single time points (5 or 10 min), or was determined by

fitting parameters to the experimental data. The Cl⁻ fluxes were calculated as $k \text{Cl}_i^-$.

Statistical analysis

The data are shown as means ± SEM. Student's t test was used to evaluate the statistical significance. The significance level was set at $P < 0.05$.

The authors have read and the experiments comply with the policies and regulations of *The Journal of Physiology* given by Drummond (2009).

Results

³⁶Cl⁻ movement and distribution

The rate constant of ³⁶Cl⁻ exchange in the cells under normal conditions was in the range 0.12–0.19 min⁻¹ (Fig. 1, Table 1), a value similar to that of other proliferating cells (Aull *et al.* 1977; Hoffmann *et al.* 1979; Levinson, 1985; Ladoux *et al.* 1987). Incubation of cells in the medium with ³⁶Cl⁻ for 60–90 min is therefore sufficient to reach a balanced ³⁶Cl⁻ distribution. The rate constant of ³⁶Cl⁻ exchange in cells undergoing apoptosis induced by 1 μM STS increased by a factor of 1.3–1.5 for 4 h. The slower release of ³⁶Cl⁻ into the Na⁺-free and Cl⁻-free NMDG–glutamic medium in comparison with the release in standard RPMI medium is usually taken as an indication that some portion of the Cl⁻ efflux relates to the Cl⁻/Cl⁻ exchange or cotransport pathways (Hoffmann *et al.* 1979; Simchowicz & De Weer, 1986; Simchowicz *et al.* 1986). The intracellular Cl⁻ content calculated on the basis of a steady-state ³⁶Cl⁻ distribution fell by a factor of 1.7–2.2 (depending on the cell strain) during apoptosis subsequent to exposure to 1 μM STS, and by a factor of 1.4 during apoptosis following exposure to 0.2 μM STS (Table 1).

The present data on the Cl⁻ content and its changes in apoptosis induced by STS are in agreement with values obtained for U937 cells by X-ray microanalysis (Fernández-Segura *et al.* 1999; Arrebola *et al.* 2005a, 2005b, 2006). The steady-state influx and efflux of Cl⁻ was in the range 21–43 μmol g⁻¹ min⁻¹ (Table 1). The difference between influx and efflux in STS-treated cells, i.e. the net Cl⁻ flux, was estimated by an integration of the decrease of the intracellular Cl⁻ content over apoptosis lasting 4 h. The resulting value of about 0.4–0.5 μmol g⁻¹ min⁻¹ was small in comparison with the 'turnover' flux. The state of the cells after incubation with STS for 4 h is therefore essentially balanced with regard to the Cl⁻ distribution. A similar balance was found for the Na⁺ and K⁺ (Rb⁺) fluxes in U937 cells during STS-induced apoptosis (Vereninov *et al.* 2007). The flux balance equations were used to analyse the changes of the Cl⁻, Na⁺ and K⁺ transport in apoptosis.

Table 1. Ion and water balance in U937 cells under normal conditions (Control) and during apoptosis caused by exposure to 0.2 or 1 μM staurosporine for 4 h (STS)

	Cells 1a		Cells 1b		Cells 2		Cells 3	
	Control	STS 1	Control	STS 0.2	Control	STS 0.2	Control	STS 1
Cl_i^- ($\mu\text{mol g}^{-1}$)	229 \pm 10 (14)	133 \pm 10 (14)	225 \pm 7 (32)	158 \pm 5 (28)	253 \pm 10 (30)	186 \pm 5 (26)	224 \pm 5 (9)	104 \pm 6 (6)
k (min^{-1})	0.14 \pm 0.01 (18)	0.21 \pm 0.01 (18)	0.19 \pm 0.03 (5)	0.17 \pm 0.02 (8)	0.12 \pm 0.03 (5)	0.13 \pm 0.004 (5)	0.16 \pm 0.01 (12)	0.20 \pm 0.01 (12)
I_{Cl}^T ($\mu\text{mol min}^{-1} \text{g}^{-1}$)	32.5	27.5	42.7	26.9	30.4	24.2	34.9	21.0
K_i^+ ($\mu\text{mol g}^{-1}$)	697 \pm 30 (16)	528 \pm 20 (16)	586 \pm 9 (34)	510 \pm 10 (28)	646 \pm 7 (31)	429 \pm 20 (26)	617 \pm 8 (9)	484 \pm 16 (9)
Na_i^+ ($\mu\text{mol g}^{-1}$)	213 \pm 9 (16)	282 \pm 2 (16)	138 \pm 3 (34)	151 \pm 7 (28)	136 \pm 4 (31)	241 \pm 20 (26)	174 \pm 8 (9)	220 \pm 14 (9)
Water (ml g^{-1})	5.52 \pm 0.13 (4)	4.55 \pm 0.06 (4)	5.64 \pm 0.1 (8)	5.00 \pm 0.07 (8)	5.76 \pm 0.2 (8)	4.96 \pm 0.11 (8)	5.60 \pm 0.04 (3)	4.34 \pm 0.19 (2)
Water decrease (%)		-17.6		-11.3		-13.9		-22.5
Cell density (g ml^{-1})	1.048 \div 1.055	1.055 \div 1.064	1.046 \div 1.055	1.052 \div 1.059	1.045 \div 1.054	1.053 \div 1.059	1.048 \div 1.052	1.059 \div 1.066
I_{Rb}^T ($\mu\text{mol min}^{-1} \text{g}^{-1}$)	1.88 \pm 0.08 (23)	1.04 \pm 0.07 (23)	1.71 \pm 0.07 (31)	1.87 \pm 0.10 (28)	1.94 \pm 0.07 (27)	1.43 \pm 0.07 (24)	2.19 \pm 0.06 (53)	0.93 \pm 0.03 (52)
$I_{\text{Rb}}^{\text{OR}}$ ($\mu\text{mol min}^{-1} \text{g}^{-1}$)	0.30 \pm 0.02 (23)	0.33 \pm 0.01 (23)	0.27 \pm 0.01 (31)	0.44 \pm 0.03 (28)	0.72 \pm 0.04 (27)	0.69 \pm 0.05 (24)	0.42 \pm 0.01 (53)	0.27 \pm 0.01 (45)
All osmolytes (mosmol g^{-1})	1.71	1.41	1.75	1.55	1.79	1.54	1.74	1.34
Sum of ions (mmol g^{-1})	1.14	0.96	0.95	0.82	0.94	0.86	1.01	0.81
Share of ions	0.67	0.68	0.55	0.53	0.52	0.56	0.57	0.60

k , rate constant of total Cl^- exchange; I_{Cl}^T , measured total Cl^- flux under balanced Cl^- conditions; I_{Rb}^T , total Rb^+ influx in absence of ouabain; $I_{\text{Rb}}^{\text{OR}}$, Rb^+ influx in presence of 0.1 mM ouabain. Share of ions, a portion of intracellular K^+ , Na^+ and Cl^- in the total intracellular osmolytes. Data were obtained in three U937 cell strains. Indexes a , b of Cells 1 indicate independent series of experiments. Values are means \pm SEM; the number of determinations is given in parentheses.

Balance of osmolytes

Determination of cell water by measuring the cell buoyant density and the intracellular K^+ and Na^+ by flame emission, together with $^{36}\text{Cl}^-$ determination, allowed us to estimate the contribution of K^+ , Na^+ , Cl^- and other

intracellular osmolytes to apoptotic cell shrinkage. The total intracellular content of osmolytes can be calculated from the cell water content, since the total osmolarity of the intracellular medium in animal cells should be the same as that in the external solution. The percentage of cellular

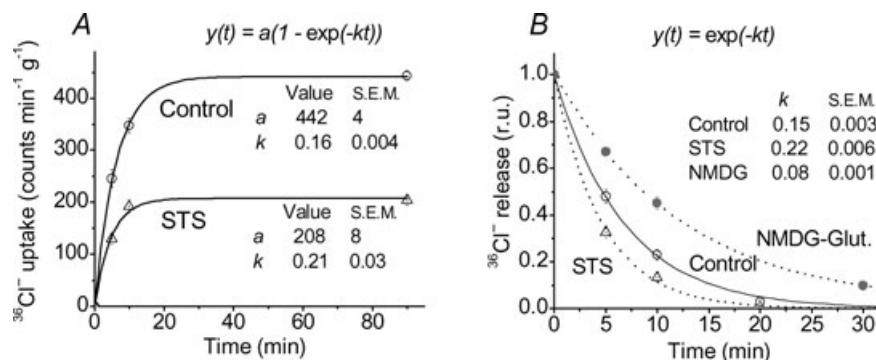


Figure 1. Time course of $^{36}\text{Cl}^-$ uptake (A) and release (B) in U937 cells undergoing apoptosis caused by exposure to 1 μM staurosporine for 4 h (STS, triangles)

A, $^{36}\text{Cl}^-$ uptake (Cells 3). B, $^{36}\text{Cl}^-$ release (Cells 1) after loading with tracer for 1.5 h in RPMI medium without (Control) or with STS given in relative units (r.u.). Filled circles show Cl^- release from control Cells 1 into NMDG-glutamic medium free of Na^+ and Cl^- . The data were approximated by equations with the parameters fitted as shown in the plots. Values are means \pm SEM, of 3–4 experiments, with duplicate or triplicate determinations.

K⁺, Na⁺ and Cl⁻ in the total amount of all osmolytes under control conditions at an external osmolarity of 310 mosmol l⁻¹ varied from 67% in Cells 1b to 52% in Cells 2 (share of ions in Table 1). The other 40–50% is accounted for by the ‘residual’ intracellular osmolytes. The bulk decrease in intracellular osmolytes in apoptosis of the cells, determined from the drop in cell water content, was 0.3–0.4 mosmol (g protein)⁻¹ in the cells treated with 1 μM STS, and was 0.2–0.25 mosmol (g protein)⁻¹ following treatment with 0.2 μM STS. This decrease resulted from the loss of K⁺, Cl⁻ and ‘residual’ intracellular osmolytes, and the opposing Na⁺ uptake (Fig. 2). Approximately 30–60% of the loss was due to K⁺, 20–30% to Cl⁻ and 20–40% to residual intracellular osmolytes.

An increase in the cellular Na⁺ content is a characteristic feature of apoptosis. This reduces the shrinkage caused by the loss of K⁺, Cl⁻ and other intracellular osmolytes. An increase in intracellular Na⁺ in apoptosis of U937 cells caused by etoposide is sufficient to balance in full the loss of K⁺, Cl⁻ and other osmolytes, and to prevent cell shrinkage (Yurinskaya *et al.* 2005a).

Changes of channels and transporters in apoptotic cells based on the overall balance of the Cl⁻, K⁺ and Na⁺ fluxes

Modelling of the overall balance of the Cl⁻, K⁺ and Na⁺ fluxes. The values of the Cl⁻, K⁺ and Na⁺ concentrations and the Cl⁻ and K⁺ fluxes given a balanced ion distribution

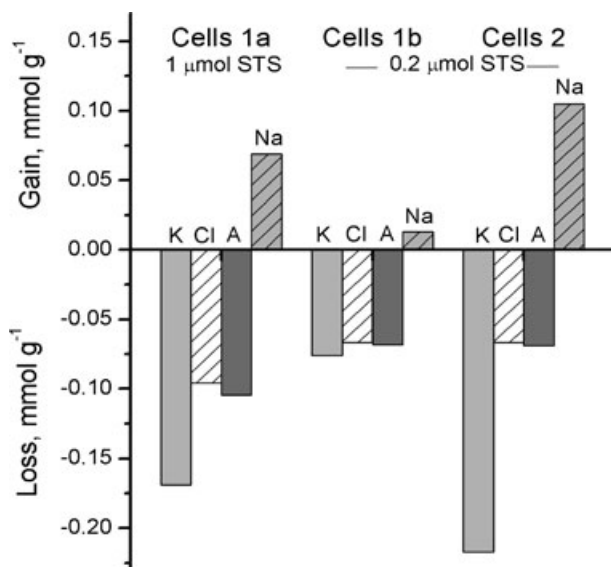


Figure 2. Loss of K⁺, Cl⁻, residual osmolytes (A) and gain of Na⁺ in U937 cells following induction of apoptosis by 1 or 0.2 μM staurosporine for 4 h (STS)

Residual intracellular osmolytes were calculated by subtracting the K⁺, Na⁺ and Cl⁻ content from total intracellular osmolytes: A = 310 × Water - (K⁺ + Na⁺ + Cl⁻). See note to Table 1 for further details.

allow us to compute all net fluxes of Cl⁻, K⁺ and Na⁺ via distinct pathways across the cell membrane provided that a set of pathways is specified (see Appendix). The minimal model should consist of the Na⁺/K⁺ pump, Cl⁻, K⁺ and Na⁺ channels, and electroneutral NKCC or NC cotransport pathways. The stoichiometry of NKCC cotransport is assumed to be 1:1:2 (Russell, 2000). Na⁺-Cl⁻ (NC) cotransport with 1:1 stoichiometry may be performed by a single transport protein, like thiazide-sensitive Na⁺-Cl⁻ cotransporter (Gamba, 2005), or by two functionally coupled exchangers, e.g. NHE and Cl⁻/HCO₃⁻ (Garcia-Soto & Grinstein, 1990; Hoffmann *et al.* 2009). Active transport of Cl⁻ due to cotransport with Na⁺ or with Na⁺ and K⁺ is required because the balanced distribution of Cl⁻ can deviate from electrochemical equilibrium.

When is the simultaneous balance of Cl⁻, K⁺ and Na⁺ fluxes possible? Analysis of the flux balance equation shows that the flux balance for each species of monovalent ions, Cl⁻, Na⁺ and K⁺, can be accomplished in the model with NKCC cotransport at any value of the total measured Cl⁻ flux, I_{Cl}^T . However, in the model with NC the flux balance may exist only if the sum of the unidirectional fluxes via cotransporter and channels, I_{Cl}^t , does not exceed a certain limit. This limit depends on the balance of the Na⁺ fluxes because the Na⁺ flux available for NC cotransport becomes deficient under certain conditions. The limit of I_{Cl}^t depends on the cell properties and can be calculated from the data in Table 1 (see Appendix).

An important point is that the measured total Cl⁻ flux, I_{Cl}^T , in most of the studied cells exceeded significantly the limit of I_{Cl}^t calculated for the model with NC (Fig. 3). The difference between the measured value I_{Cl}^T and calculated

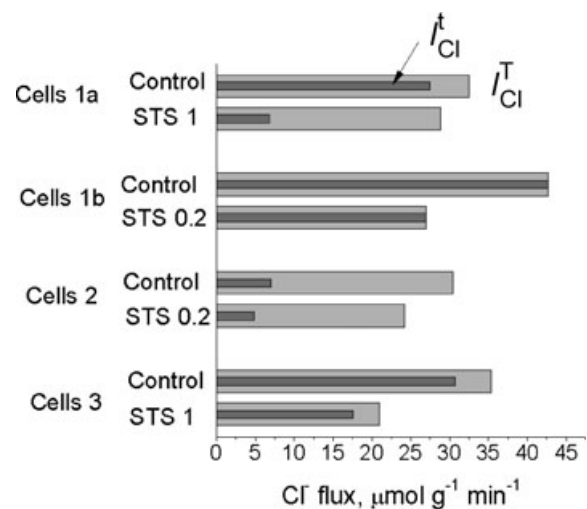


Figure 3. Total measured Cl⁻ flux under the balanced state, I_{Cl}^T , and calculated limit of unidirectional flux via channels and NC cotransport, I_{Cl}^t , in normal (Control) and apoptotic (STS 1, STS 0.2) cells

value I_{Cl}^T varies in studied cells over a rather wide range. In Cells 1b there was a small difference. The discrepancy between I_{Cl}^T and I_{Cl}^t in other cases could be caused by two reasons. One is that the NC model is inadequate. The second is that some portion of the measured Cl^- flux consists in a coupled Cl^-/Cl^- exchange with zero net flux. The existence of the similar exchange fluxes has been postulated rather long ago (see for references Hoffmann *et al.* 1979). The statement 'the steady-state isotope fluxes could not be used to measure leak permeability or active transport, since a large portion of the flux can be exchange diffusion' (Hofmann, 2001) does describe the difficulty but it does not address it. The effect of NMDG–glutamic medium on the rate of Cl^- release from U937 cells indicates the Cl^-/Cl^- exchange could take place in studied cells irrespective of the assumed cotransport model. Therefore, further analysis was performed under various assumptions on the relationship between the Cl^-/Cl^- exchange component $I^{Cl/Cl}$ and the fluxes via pathways capable of net ion transfer, i.e. channels and cotransporters.

Figure 4 shows Cl^- influx (I) and efflux (J) via distinct pathways in some of the cells calculated for the model with NKCC or NC as a function of $I^{Cl/Cl}$ at several chosen values. If $I^{Cl/Cl}$ accounts for a large part of the total Cl^- flux then the residual fluxes via channels and cotransporters taken

together are small, and vice versa. Cells 2 demonstrate that no less than 23 of 30 units of the measured Cl^- flux should be accounted for by the coupled Cl^-/Cl^- exchange if the NC model is considered (see also Fig. 3). The imbalance of the Cl^- influx and efflux through channels, as well as via cotransporters, depends on the type of cotransporter in the model and cell properties. When the imbalance is small, a significant part of the self-exchange Cl^- flux should be attributed to the channels or cotransporters, but not to a coupled Cl^-/Cl^- exchange (Fig. 4A). In this case the Cl^- distribution is close to the electrochemical equilibrium, the forward and backward fluxes through the channels are equal and cannot be distinguished from the coupled Cl^-/Cl^- exchange. Separation of the Cl^-/Cl^- equivalent exchange via the coupled Cl^-/Cl^- exchange and through the channels therefore appears to be a matter of convention. The imbalance of the channel influx and efflux is more pronounced when the model with NC is considered (Fig. 4C and D). It is true both for channel and cotransport fluxes. An example of small net flux due to NKCC cotransport is shown in Fig. 4A. In this case an integral electrochemical potential difference that moves Cl^- , Na^+ and K^+ via the NKCC pathway, $\Delta\mu_{NKCC}$, was as small as 7.1 mV, whereas in the other cases (Fig. 4B) it could reach 33 mV ($\Delta\mu_{NKCC} = RT/F \ln\{[Na]_i [K]_i [Cl]_i [Cl]_i / ([Na]_o [K]_o [Cl]_o [Cl]_o)\}$).

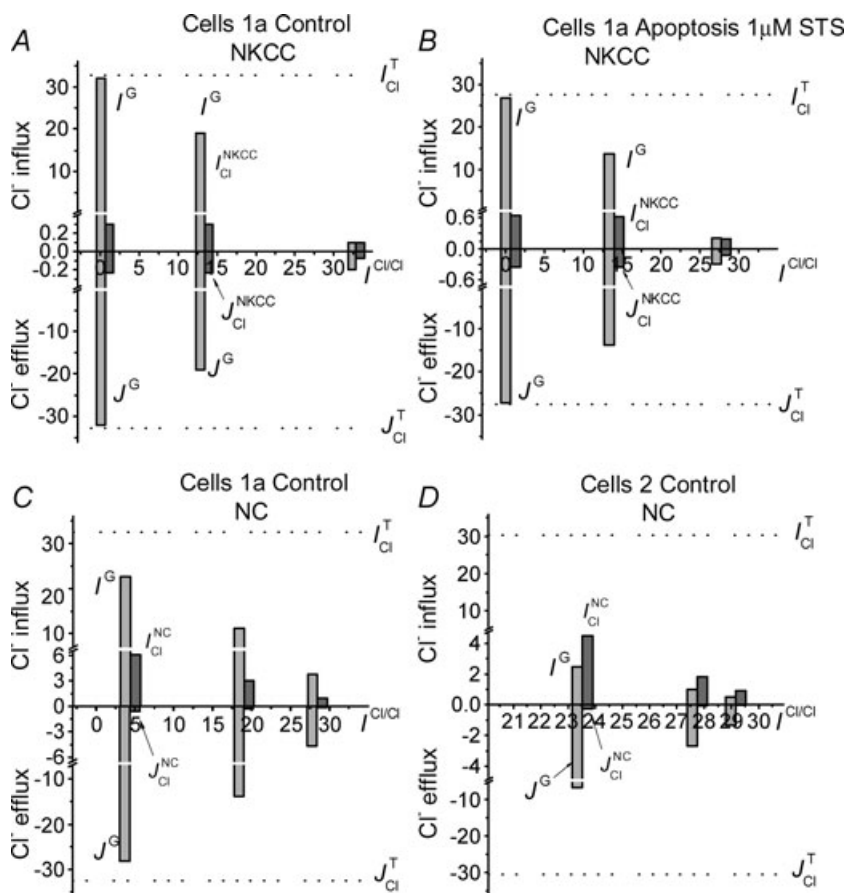


Figure 4. Relationship between Cl^- influx (I) and efflux (J) via different pathways in normal and apoptotic U937 cells as a function of the assumed $I^{Cl/Cl}$ value for the models with NC or NKCC cotransport I_{Cl}^T , total Cl^- flux measured under the balanced state (shown by dotted line); light grey columns, fluxes through channels (I^G , J^G); dark grey columns, fluxes related to cotransport through NC (I_{Cl}^{NC} , J_{Cl}^{NC}) or NKCC (I_{Cl}^{NKCC} , J_{Cl}^{NKCC}). Basic data for calculations are taken from Table 1. Fluxes are given in $\mu\text{mol min}^{-1}$ (g protein) $^{-1}$.

The NKCC cotransport fluxes are small in comparison with the measured total Cl⁻ flux I_{Cl}^{T} . The flux $I_{\text{Cl}}^{\text{NKCC}}$ in most of the cells we studied did not exceed $0.6 \mu\text{mol g}^{-1} \text{min}^{-1}$ except for Cells 2 (approximately $2 \mu\text{mol g}^{-1} \text{min}^{-1}$), whereas the measured total Cl⁻ flux in the studied cells was in the range $21\text{--}43 \mu\text{mol g}^{-1} \text{min}^{-1}$ (Table 1). This indicates the importance of the approach developed here as it would be difficult to detect such small fractional flux experimentally. The flux $I_{\text{Cl}}^{\text{NC}}$ is also small relative to the measured Cl⁻ flux. The maximal values of $I_{\text{Cl}}^{\text{NC}}$ were about $3\text{--}6 \mu\text{mol g}^{-1} \text{min}^{-1}$, so that they did not exceed 20% of the measured Cl⁻ flux. The NC and NKCC fluxes are very important in maintaining the balance between total Cl⁻ influx and efflux under the non-equilibrium Cl⁻ distribution. At the same time the changes in these pathways are not critical for apoptotic cell shrinkage, as we supposed earlier (Vereninov *et al.* 2007). Apoptosis of Cells 1 and 3 with similar shrinkage was accompanied by changes of these fluxes in opposing directions. There were no changes in the cotransport Cl⁻ fluxes in apoptosis induced by $0.2 \mu\text{M}$ STS in Cells 2, whereas apoptosis of Cells 1b was accompanied by a small increase in $I_{\text{Cl}}^{\text{NKCC}}$ and I^{NC} (data not shown).

Effects of blockers. Several experiments were performed to determine the effects on Cl⁻ fluxes of known channel blockers, such as NPPB (0.25 mM), DIDS (0.5 mM) and the NKCC cotransport inhibitor bumetanide (0.05 mM). Bumetanide had no obvious effect on the Cl⁻ flux. This corresponds to the minor contribution of NKCC to the total Cl⁻ flux. A small effect of bumetanide has been observed on Rb⁺ fluxes, the K/Na ratio and the cation content in U937 cells (Vereninov *et al.* 2008). NPPB and DIDS induced a decrease in the Cl⁻ rate constant by factors of 2 and 1.5, respectively (Fig. 5). The effects of NPPB and DIDS were not additive and can be attributed mainly to their identical target, the Cl⁻ channels. Accordingly, about half of the total unidirectional Cl⁻ flux can be defined as the channel flux. The residual part, which is bumetanide+DIDS+NPPB resistant, has not yet been specified. The contribution of channels to the Cl⁻ flux in U937 cells was greater than in other cells, e.g. in Ehrlich ascites tumour cells, where it approaches 5% of the total Cl⁻ influx (Hoffmann *et al.* 1979, 2009; Hoffmann, 1982). The NPPB-inhibitable Cl⁻ flux was not increased during apoptosis. This suggests that there was no activation of Cl⁻ channels in the present experiments. Long-term incubation (1.5 or 4 h) of U937 cells with DIDS or NPPB was not followed by significant (>10%) changes in intracellular Cl⁻, K⁺ or Na⁺ content. The increase in the buoyant density of cells, i.e. cell shrinkage, caused by $1 \mu\text{M}$ STS, was less pronounced if cells were treated by STS with addition of NPPB.

Integral channel permeability of the cell membrane for Cl⁻. Goldman's formalism was used for description of 'electroconductive' or 'channel' ion pathways as a whole (see Appendix). Figure 6 shows that the calculated values of permeability coefficient P_{Cl} depend linearly on the Cl⁻ flux mediated by channels and cotransport I_{Cl}^{T} . The values of P_{Cl} obtained for the NKCC (large symbols) and for the NC (small symbols) models proved to be almost coincident at one and the same I_{Cl}^{T} . We can conclude therefore that estimation of P_{Cl} does not depend practically on the assumed cotransport model (at least if a specific link between cotransport model and the value of the coupled Cl⁻/Cl⁻ flux is not hypothesized). More difficult is to settle the question of how P_{Cl} is altered in apoptosis. It should be known what the subdivision of the total measured Cl⁻ flux into the fluxes I_{Cl}^{T} and $I_{\text{Cl}}^{\text{Cl/Cl}}$ in apoptotic and normal cells is. Apoptotic volume decrease is currently explained often by the opening of the Cl⁻ channels (D'Anglemont de Tassigny *et al.* 2004; Ise *et al.* 2005; Okada *et al.* 2009; Poulsen *et al.* 2010). Our calculations show that significant increase in P_{Cl} in apoptotic cells if it occurs should be accompanied by a no less significant decrease in the coupled Cl⁻/Cl⁻ flux. However, the values of P_{Cl} obtained for the NKCC and for the NC models given identical coupled Cl⁻/Cl⁻ exchange are similar, and in the apoptotic cells they are equal to or lower than those in control cells (Fig. 6D–F).

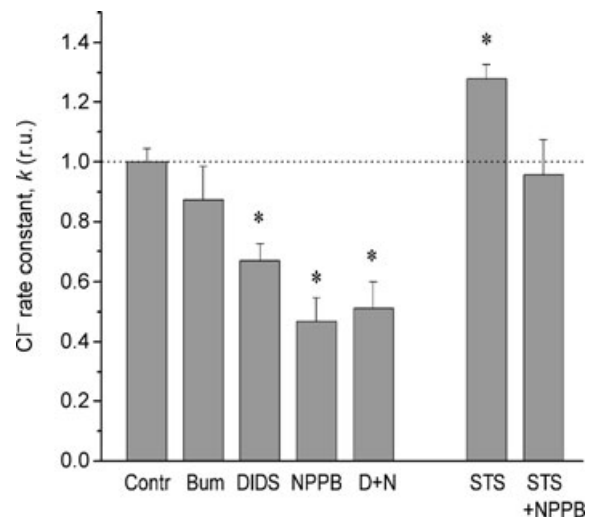


Figure 5. Effects of blockers on the $^{36}\text{Cl}^-$ exchange rate constant in U937 cells

Bumetanide (Bum, 0.05 mM), DIDS (0.5 mM) and NPPB (0.25 mM) were added in RPMI medium, 20 min before $^{36}\text{Cl}^-$. Simultaneous addition of DIDS and NPPB is marked D+N. Rate constants were calculated as $k = -\ln(1 - y_0/y_\infty)/t$, relative units (r.u.). The data were obtained in Cells 3. Means \pm SEM for 3–4 experiments, with duplicate determinations. Significant differences from controls are shown by an asterisk ($P < 0.05$).

Integral channel permeability of the cell membrane for Na^+ . The solution of the flux balance equation made it possible to calculate P_{Na} without direct measurement of the Na^+ fluxes, supposing only that the balanced Na^+

distribution holds and that the ratio of the Na^+ and K^+ fluxes via the pump is 3:2. Figure 6G–I show how P_{Na} changes during apoptosis in models with NKCC and NC cotransport as a function of I_{Cl}^t . The values of P_{Na}

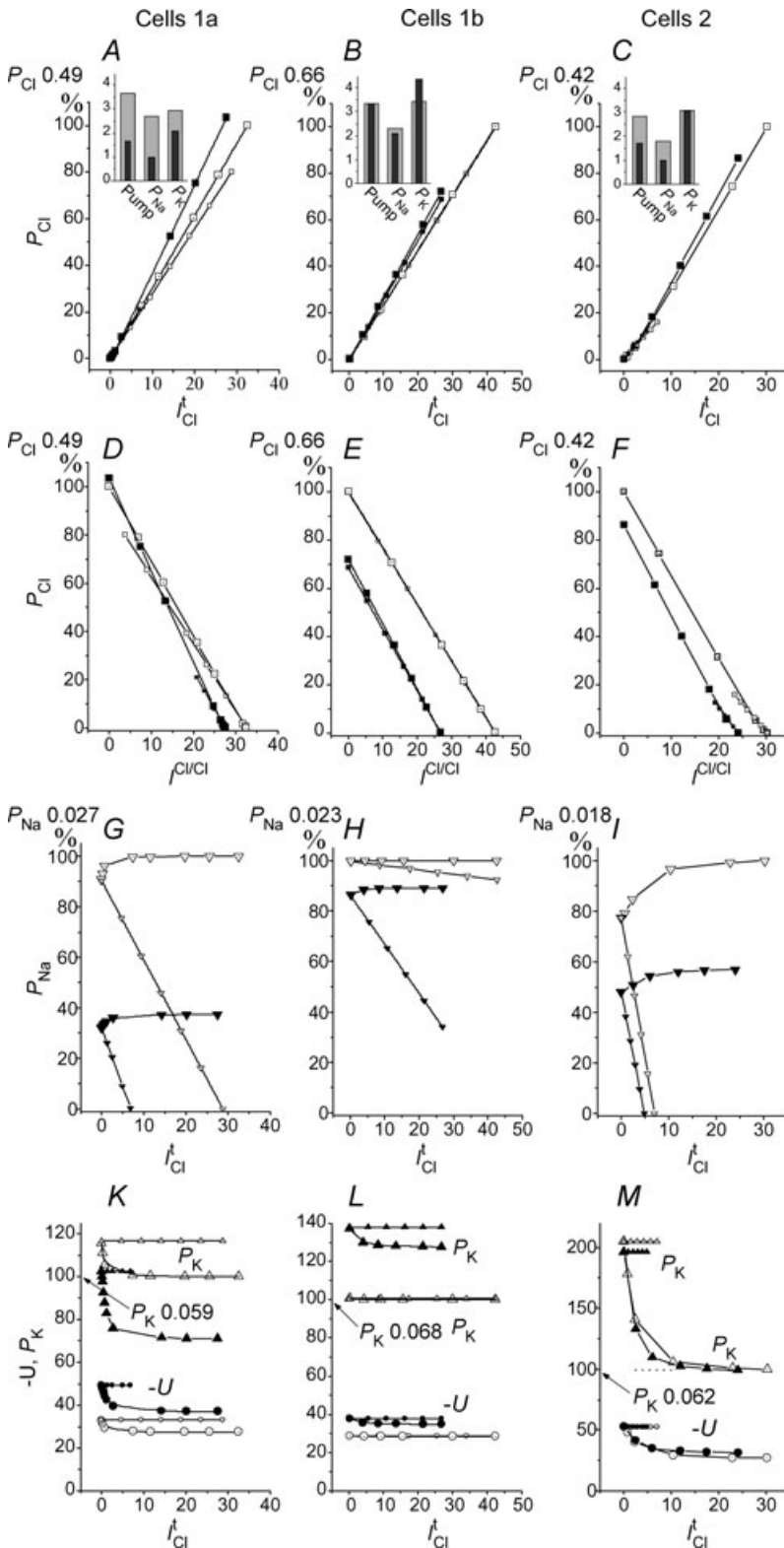


Figure 6. Permeability coefficients P_{Cl} , P_{Na} , P_{K} and membrane potential U in normal (open symbols) and apoptotic (filled symbols) U937 cells calculated for the models with NKCC (large symbols) or NC (small symbols) cotransporters

Data are plotted as a function of Cl^- influx related to channels and cotransporters, I_{Cl}^t , or to the coupled Cl^-/Cl^- exchange, $I_{\text{Cl}}^t/\text{Cl}^-$. Basic data are taken from Table 1. Apoptosis in Cells 1a was induced by $1 \mu\text{M}$ whereas in Cells 1b and Cells 2 by $0.2 \mu\text{M}$ STS. P_{Cl} , P_{Na} and P_{K} are normalized by using as reference the values obtained for NKCC model with zero Cl^-/Cl^- exchange. The reference values in $\text{ml g}^{-1} \text{min}^{-1}$ are shown in the left upper corner of the plots. Insets: pump flux (I_{P}^p , $\mu\text{mol min}^{-1} \cdot \text{g}^{-1}$), P_{Na} ($\text{ml g}^{-1} \text{min}^{-1} \times 100$) and P_{K} ($\text{ml g}^{-1} \text{min}^{-1} \times 50$) calculated for the NKCC model at zero $I_{\text{Cl}}^t/\text{Cl}^-$; light grey columns are control cells; dark grey columns, apoptotic cells.

calculated for the NKCC model (large triangles) remain nearly constant over a wide range of I_{Cl}^t . The P_{Na} level in apoptosis of Cells 1a and 3 (data not shown) induced by 1 μM STS is 2.5–3.0 times less than in normal cells. For milder apoptosis (Cells 2) induced by 0.2 μM STS, P_{Na} decreases by a factor of 1.6. However, P_{Na} in apoptosis induced by 0.2 μM STS in Cells 1b decreases by only about 10% (compare filled and open large triangles in Fig. 6H). The slight decrease of P_{Na} in this case correlates with the absence of changes in the pump fluxes I_K^p (see inset in Fig. 6B). We can suppose that a decrease of P_{Na} in apoptosis is coupled to a decrease in the pump fluxes. The decrease in the integral channel permeability of membrane for Na⁺ when the pump is suppressed is useful, because it reduces the gain of Na⁺ and the concomitant cell swelling. This phenomenon is crucial to apoptotic cell shrinkage when the pump is inhibited.

The values of P_{Na} calculated for the model with NC (Fig. 6G–I, small triangles) depend significantly on the assumed relationship between I_{Cl}^t and $I^{Cl/Cl}$ in the measured total Cl⁻ flux I_{Cl}^t . The situation is similar to that for P_{Cl} . Comparison of the data calculated at identical $I^{Cl/Cl}$ indicates that P_{Na} in apoptosis is lower than that for cells in the normal state for all cases studied except Cells 2 (data not shown). The absolute values of P_{Na} calculated for the models NC and NKCC differ significantly from each other because of the differing contribution of the I^{NC} and I^{NKCC} fluxes to the total balance of Na⁺ fluxes.

Integral channel permeability of the cell membrane for K⁺. Changes in the ouabain-sensitive and ouabain-resistant Rb⁺ influx during apoptosis of U937 cells induced by STS have been found to depend on the depth of apoptosis and cell properties (Vereninov *et al.* 2008). The permeability coefficient P_K was calculated in the present study using the equations set out in the Appendix. The P_K reflects alterations of channel activity more accurately than the flux value because the effect of variations in the membrane potential is eliminated. Figure 6 demonstrates that only the apoptosis in Cells 1b caused by 0.2 μM STS was associated with an increase in P_K . In other cells the P_K remained unchanged (mild apoptosis of Cells 2), or decreased (more severe apoptosis in Cells 1 and 3). Consequently, cell shrinkage in apoptosis of the cells we studied here occurs mostly without an increase in P_K . An increase in P_K in apoptosis was observed when the pump flux remained unchanged (Vereninov *et al.* 2008). No changes were observed in Rb⁺ efflux during apoptosis of U937 cells following treatment with 1 μM STS in previous experiments, in which the Rb⁺ efflux was studied after 24 h incubation of cells in RPMI medium with 1 mM Rb⁺ (Vereninov *et al.* 2007). The conclusion concerning minute changes of P_K holds even if rectification in K⁺ channels is

allowed for in the model (Rubashkin *et al.* 2010). Insets in Fig. 6A–C illustrate the relationship between changes in the pump flux (I_K^p), P_K and P_{Na} in different apoptotic cells observed in the present study.

Membrane potential. The values of the membrane potential calculated according to Ussing (1949) from the measured fluxes and distribution of Rb⁺ are shown in Fig. 6K–M. The membrane potential in the U937 cells was in the range of –30 to –50 mV. This value is consistent with the measured and calculated values obtained for various proliferating cells (Hoffmann *et al.* 1979; Lambert *et al.* 1989; Wonderlin *et al.* 1995; Ouadid-Ahidouch *et al.* 2004). The calculated membrane potential in the model with NC does not depend on the assumed portion of $I^{Cl/Cl}$ in the measured total Cl⁻ flux. In contrast, in the NKCC model a portion of the Cl⁻ flux is coupled to the K⁺ flux in the NKCC cotransporter. The ratio of channel K⁺ (Rb⁺) efflux to influx is therefore changed. Consequently, the membrane potential is changed. An increase in membrane potential becomes apparent when the flux $I^{Cl/Cl}$ exceeds 85% of the total measured flux I_{Cl}^t .

The calculated membrane potential of all cells, except Cells 2, was hyperpolarizing by 10–15 mV in apoptosis. For Cells 2 the potential did not change during apoptosis. These results differ from previous findings (Franco *et al.* 2006), and further studies are required to determine whether cell depolarization occurs in more severe apoptosis or whether the cell model we have used here is incomplete. A more complex model, including cotransport KCC and the assumption that apoptosis is accompanied by KCC decrease, sees cell depolarization (Rubashkin *et al.* 2010).

Discussion

It is clear that the monovalent ion channels and transporters are involved in apoptosis. Numerous studies, mostly electrophysiological, indicate that apoptosis is associated with changes to various ion channels and transporters. Conversely, alteration of the channels and transporters can influence apoptosis. It is important to distinguish the role of monovalent ions in signalling related to apoptosis, and their role as osmolytes responsible for preventing osmotic bursting of a cell during apoptosis. This second role has not been investigated in detail. Many studies provide information only on one species of ions or a single ion pathway, and do not consider the overall ion and water balance of the cell. Recent progress has been made by elemental X-ray microanalysis of cells undergoing apoptosis (Fernandez-Segura *et al.* 1999; Skepper *et al.* 1999; Arrebola *et al.* 2005a,b, 2006). Quantitative changes in the joint K, Na, Cl, P, Mg and S content in U937 cells undergoing apoptosis

due to exposure to staurosporine or other agents was estimated in these works. Unfortunately there was no determination of cell water, so that the analysis of the ion and water balance in apoptotic cells is not complete. Further progress was achieved by Poulsen *et al.* (2010), who determined in apoptotic Ehrlich ascites tumour cells the K^+ , Na^+ , Cl^- levels, 'ninhydrin-positive' substances and cell water. In the present study we have aimed to determine all major players in the apoptotic disturbance of osmotic balance in human lymphoma U937 cells treated with STS. The amount of intracellular osmolytes other than K^+ , Na^+ and Cl^- was calculated by subtraction of the monovalent ion content from the total intracellular osmolyte content. The latter was calculated in turn from the amount of cell water and the total osmolarity of the extracellular (and hence intracellular) medium. The errors in this procedure are critical for the estimation of 'residual' intracellular osmolytes, and the information obtained should be regarded as approximate. Our findings nevertheless indicate that the apoptotic decrease in the intracellular amount of osmolytes defined as 'residual' is comparable with the decrease in Cl^- content. The decrease in Cl^- , K^+ and 'residual' intracellular osmolytes is responsible for the total decrease in cell water, whereas the increase in Na^+ plays an opposite role. The decrease in Cl^- , K^+ and 'residual' intracellular osmolytes in U937 cells undergoing apoptosis following exposure to etoposide is fully counterbalanced by an increase in Na^+ content, and no cell shrinkage occurs (Yurinskaya *et al.* 2005a).

Analysis of 'isosmotic' cell volume regulation in apoptosis is based mainly on analogy with 'anisomotic' cell volume regulation by such reactions as regulatory volume decrease (RVD) and regulatory volume increase (RVI). This is why the term apoptotic volume decrease (AVD) was coined (Maeno *et al.* 2000; Okada & Maeno, 2001; Burg *et al.* 2006; Okada *et al.* 2006; Bortner & Cidlowski, 2007; Lambert *et al.* 2008; Lang *et al.* 2008; Hoffmann *et al.* 2009). In fact the RVD is usually studied as a short-term response to the acute osmotic disturbance associated with the sharp (up to 1.5 times) increase in the cell volume, whereas long-term apoptotic cell shrinkage is a drift of the essentially balanced ion and water distribution. This is associated with a decrease in the cell volume of about 15–25%. To study apoptotic cell shrinkage we therefore applied the flux balance equations to the double Donnan system with the Na^+/K^+ pump, the Na^+ , K^+ and Cl^- electroconductive channels, NKCC or NC cotransport, and Cl^-/Cl^- exchange. The present paper is based on this approach.

Estimation of the Cl^- flux related to the Cl^-/Cl^- exchange pathway is crucial in calculating the total balance of the unidirectional Cl^- , Na^+ and K^+ fluxes. Because of difficulties in the experimental detection of the coupled Cl^-/Cl^- flux under a balanced ion distribution, the

calculations were performed for different values of the Cl^-/Cl^- flux. Significant conclusions can be drawn by modelling the total ion flux balance in the cells under study in spite of the uncertainty in the determination of the Cl^-/Cl^- flux and the simplistic mathematical model. A decrease in integral channel permeability of membrane for Na^+ is crucial to cell shrinkage in apoptosis accompanied by a decrease in the sodium pump fluxes. This was seen in the severe apoptosis of U937 cells caused by $1 \mu M$ STS (4 h). No significant changes occurred in the integral channel permeability of membrane for K^+ in these cells. On the other hand, mild apoptosis induced by $0.2 \mu M$ STS in cells of one of the cell strains studied was associated with an increase in integral channel permeability of membrane for K^+ without change in the pump and the Na^+ channels. Our calculations showed that the net Cl^- flux through the channels in the cells we studied was small compared to the total flux measured by $^{36}Cl^-$. This implies that the opposite active net Cl^- flux due to cotransport was also small. This is why Cl^- cotransport fluxes are difficult to reveal by inhibitors.

Finally, in view of the limited role of the Cl^- and K^+ channels in apoptotic cell shrinkage, and the abundant electrophysiological evidence for their involvement in apoptosis, we expect that there is a further role of electroconductive channels in apoptosis. This could be connected with monitoring of the membrane potential in some as yet unknown transient apoptotic processes.

Conclusions

(1) The integral decrease in the amount of intracellular osmolytes underlying apoptotic cell dehydration, by about 20%, is due to the loss of K^+ and Cl^- (56–72% of all osmolytes going out of the cell) and also some unidentified intracellular osmolytes (44–28%) and the gain of Na^+ , which counterbalances 20–25% of the ($K^+ + Cl^-$) loss.

(2) The state of the cells after incubation with $1 \mu M$ STS for 4 h should be considered as almost balanced with respect to the Cl^- , Na^+ and K^+ distributions. The values of P_{Cl} , P_{Na} , P_K and the NKCC and NC cotransport fluxes can be obtained by solving the flux balance equations if the cellular Cl^- content and fluxes, the K^+ , Na^+ , water content and the ouabain-sensitive and -resistant Rb^+ fluxes are known.

(3) The calculated values of P_{Cl} and NKCC and NC cotransport fluxes depend strongly on the portion of the coupled Cl^-/Cl^- exchange component in the Cl^- fluxes. This component could not be measured for a balanced ion distribution. Useful conclusions can nevertheless be made by modelling ion homeostasis irrespective of the exchange component value. These conclusions are as follows: (1) balance of Cl^- , Na^+ and K^+ fluxes can be accomplished

in the model with NKCC cotransport at any share of the Cl⁻/Cl⁻ exchange flux in the total measured Cl⁻ flux, whereas flux balance in the model with NC is possible only if the sum of unidirectional Cl⁻ cotransport and channel fluxes does not exceed a certain limit; (2) the values of P_{Cl} obtained for the NKCC and for the NC models given identical Cl⁻ exchange are similar, and in the apoptotic cells they are equal to or lower than those in control cells.

(4) The value of P_{Na} in apoptosis induced with 1 μM STS, which is accompanied by suppression of the pump, is lower than in normal cells by a factor of 2.5–3.0. In contrast, P_{Na} in milder apoptosis induced by 0.2 μM STS with no pump suppression decreases only by about 10%, although the channel permeability of membrane for K⁺ increases significantly in this case. The fall in integral channel permeability of cell membrane for Na⁺ is crucial in preventing cell swelling during apoptosis accompanied by suppression of the pump.

(5) Direct influence of the monovalent ion channels on the cell water balance cannot explain all of the observed effects of monovalent ions in apoptosis. Involvement of these channels in monitoring of the membrane potential is likely, in some as yet unknown transient apoptotic processes.

Appendix

A minimal cell model based on the known principles (Jakobsson, 1980; Lew & Bookchin, 1986; Hoffmann, 1987; Vereninov *et al.* 2004, 2006) is considered where Na⁺, K⁺ and Cl⁻ net fluxes into and out of the cell are balanced due to parallel functioning of the Na⁺/K⁺ pump, electroconductive channels, and NKCC or NC cotransport. Equations (A1.1)–(A1.3) represent the flux balance (symbols are specified in Definitions)

$$P_{Na}u \frac{\{[Na]_i \exp(u) - [Na]_o\}}{1 - \exp(u)} + J_{Na}^P + I_{Na}^{NC} (1 - f_{NC}) + I_{Na}^{NKCC} (1 - f_{NKCC}) = 0, \tag{A1.1}$$

$$P_Ku \frac{\{[K]_i \exp(u) - [K]_o\}}{1 - \exp(u)} + I_K^P + I_K^{NKCC} (1 - f_{NKCC}) = 0, \tag{A1.2}$$

$$P_{Cl}u \frac{\{[Cl]_i - [Cl]_o \exp(u)\}}{1 - \exp(u)} + I_{Cl}^{NC} (1 - f_{NC}) + I_{Cl}^{NKCC} (1 - f_{NKCC}) = 0. \tag{A1.3}$$

The first members in these equations are the net fluxes through the channels, where P_{Na}, P_K and P_{Cl} are integral channel permeability coefficients according to Goldman (1943). J_{Na}^P and I_K^P are Na⁺ efflux and K⁺ influx via the Na⁺/K⁺ pump connected by the relationship J_{Na}^P = -1.5 · I_K^P. The values I_{Cl}^{NC} and I_{Cl}^{NKCC} are the influxes of Cl⁻ due to NC and NKCC cotransport. (I_{Cl}^{NC}f_{NC}) and (I_{Cl}^{NKCC}f_{NKCC}) are the Cl⁻ effluxes via cotransporters. It is assumed that f_{NKCC} and f_{NC} are the simple functions of concentrations

$$f_{NC} = [Na]_i[Cl]_i / ([Na]_o[Cl]_o), \tag{A2.1}$$

$$f_{NKCC} = [Na]_i[K]_i[Cl]_i / ([Na]_o[K]_o[Cl]_o). \tag{A2.2}$$

The stoichiometry of the NKCC cotransporter is assumed to be 1:1:2 (see references in Russell, 2000). The term NC cotransporter is a functional definition. Actually, unidirectional Na⁺-Cl⁻ cotransport with 1:1 stoichiometry may be performed by a single transport protein, like thiazide-sensitive Na⁺-Cl⁻ cotransporter (Gamba, 2005), or by two functionally coupled exchangers, e.g. NHE and Cl⁻/HCO₃⁻ (Garcia-Soto & Grinstein, 1990; Hoffmann *et al.* 2009). Hence, following relationships between Cl⁻, Na⁺ and K⁺ cotransport influxes should be held

$$I_{Cl}^{NKCC} = 2I_{Na}^{NKCC} = 2I_K^{NKCC}; I_{Cl}^{NC} = I_{Na}^{NC}. \tag{A2.3}$$

Equation (A1.3) does not include Cl⁻ influx and efflux mediated by one-for-one Cl⁻ exchanger whereas the flux measured by ³⁶Cl⁻ includes this flux. The experimental separation of this flux is difficult and analysis of the flux balance was performed under different assumptions on the value of this flux. Therefore, the total unidirectional Cl⁻ influx I_{Cl}^t via all pathways of eqn (A1.3) is introduced below for using as independent variable.

$$I_{Cl}^t = -P_{Cl}u \frac{[Cl]_o \exp(u)}{1 - \exp(u)} + I_{Cl}^{NKCC} + I_{Cl}^{NC} \tag{A3}$$

When the model includes only NC cotransport the influx I_{Cl}^{NC} and P_{Cl} are connected with I_{Cl}^t and the membrane potential u by the expressions

$$I_{Cl}^{NC} = I_{Cl}^t \left(\frac{1 - \exp(u - \varphi_{Cl})}{1 - f_{NC} \exp(u - \varphi_{Cl})} \right), \tag{A4}$$

$$P_{Cl} = I_{Cl}^t \left(\frac{1 - \exp(u)}{(-u) [Cl]_i} \right) \left(\frac{1 - f_{NC}}{1 - f_{NC} \exp((u - \varphi_{Cl}))} \right), \tag{A5}$$

where φ_{Cl} is the dimensionless Cl⁻ equilibrium potential, φ_{Cl} = ln([Cl]_i/[Cl]_o).

When the model includes only NKCC cotransport the analogous expressions for I_{Cl}^{NKCC} and P_{Cl} are held

$$I_{Cl}^{NKCC} = I_{Cl}^t \left(\frac{1 - \exp(u - \varphi_{Cl})}{1 - f_{NKCC} \exp(u - \varphi_{Cl})} \right), \quad (A6)$$

$$P_{Cl} = I_{Cl}^t \left(\frac{1 - \exp(u)}{(-u) [Cl]_i} \right) \left(\frac{1 - f_{NKCC}}{1 - f_{NKCC} \exp((u - \varphi_{Cl}))} \right). \quad (A7)$$

An important point is the determination of the membrane potential u . It can be done according to the Ussing theory provided that Rb^+ efflux and influx through channels and equilibrium potential φ_{Rb} are known (Ussing, 1949; Lambert *et al.* 1989)

$$\frac{J_{Rb}^G}{I_{Rb}^G} = -\exp(u - \varphi_{Rb}), \quad (A8)$$

where $\varphi_{Rb} = \ln([Rb]_o/[Rb]_i)$. The concentration $[Rb]_i$ is connected with $[K]_i$ by proportion $[Rb]_i = [K]_i [Rb]_o/[K]_o$. The influx I_{Rb} via the NKCC cotransporter can be expressed as $\{0.5 I_{Cl}^{NKCC} ([Rb]_o/[K]_o)\}$. The Rb^+ influx I_{Rb}^G and efflux J_{Rb}^G through the K^+ channels can be expressed as

$$I_{Rb}^G = \{I_{Rb}^T - I_{Rb}^P - 0.5 \cdot I_{Cl}^{NKCC} [Rb]_o/[K]_o\}, \quad (A9)$$

$$J_{Rb}^G = -\{I_{Rb}^T - 0.5 \cdot f_{NKCC} I_{Cl}^{NKCC} [Rb]_o/[K]_o\}, \quad (A10)$$

where I_{Rb}^T is the total measured Rb^+ influx. From eqns (A8)–(A10) follows

$$\{\exp(u - \varphi_{Rb})\} \{I_{Rb}^T - I_{Rb}^P - 0.5 \cdot I_{Cl}^{NKCC} ([Rb]_o/[K]_o)\} - \{I_{Rb}^T - 0.5 f_{NKCC} I_{Cl}^{NKCC} ([Rb]_o/[K]_o)\} = 0. \quad (A11)$$

After transferring I_{Cl}^{NKCC} from eqn (A6) into eqn (A11) the latter is transformed to an equation of second power, where $\exp(u)$ is a single unknown variable. The solution of eqn (A11) is simplified in case of the model with NC.

$$U_0 = \frac{RT}{F} \ln \left(\frac{[Rb]_o I_{Rb}^T}{[Rb]_i (I_{Rb} - I_{Rb}^P)} \right). \quad (A12)$$

When u is found, the values I_{Cl}^{NC} and I_{Cl}^{NKCC} can be obtained by using eqns (A4) and (A6). The channel Cl^- influx I_{Cl}^G and efflux J_{Cl}^G are calculated as

$$I_{Cl}^G = -P_{Cl} u \frac{[Cl]_o \exp(u)}{1 - \exp(u)}, \quad (A13)$$

$$J_{Cl}^G = P_{Cl} u \frac{[Cl]_i}{1 - \exp(u)}. \quad (A14)$$

The permeability coefficients P_{Na} , P_K and P_{Cl} are calculated from eqns (A1.1) and (A1.2) provided that potential u and influxes due to cotransport are known:

$$P_{Na} = \left(\frac{\exp(u) - 1}{u ([Na]_i \exp(u) - [Na]_o)} \right) \times \{J_{Na}^P + I_{Na}^{NC} (1 - f_{NC}) + I_{Na}^{NKCC} (1 - f_{NKCC})\}, \quad (A15)$$

$$P_K = \left(\frac{\exp(u) - 1}{u ([K]_i \exp(u) - [K]_o)} \right) \times \{I_K^P + I_K^{NKCC} (1 - f_{NKCC})\}, \quad (A16)$$

$$P_{Cl} = \left(\frac{\exp(u) - 1}{u ([Cl]_i - [Cl]_o \exp(u))} \right) \times \{I_{Cl}^{NC} (1 - f_{NC}) + I_{Cl}^{NKCC} (1 - f_{NKCC})\}. \quad (A17)$$

The upper limit for I_{Cl}^t in the model with NC cotransport can be obtained from the relationship $(I_{Cl}^t)_{max} = (I_{Cl}^G)_{max} + (I_{Cl}^{NC})_{max}$. In view of eqn (A1.1) the upper limit for I_{NC} can be calculated as $(I_{Cl}^{NC})_{max} = (-J_{Na}^P)/(1 - f_{NC})$. Therefore,

$$(I_{Cl}^t)_{max} = (P_{Cl})_{max} u_0 \frac{\{-[Cl]_o \exp(u_0)\}}{1 - \exp(u_0)} + \frac{(-J_{Na}^P)}{1 - f_{NC}} \quad (A18)$$

The dimensionless potential u_0 is calculated by eqn (A12), as $u_0 = U_0 F/RT$, for $37^\circ C$, $u_0 = U_0/(26.7)$.

The $(P_{Cl})_{max}$ can be derived from eqn (A1.3) at $I_{Cl}^{NKCC} = 0$

$$(P_{Cl})_{max} = \frac{J_{Na}^P (1 - \exp(u_0))}{u_0 ([Cl]_i - [Cl]_o \exp(u_0))}. \quad (A19)$$

Equation (A18) can be rewritten if chloride permeability from eqn (A19) is substituted

$$(I_{Cl}^t)_{max} = (-J_{Na}^P) \left\{ \frac{[Cl]_o \exp(u_0)}{[Cl]_i - [Cl]_o \exp(u_0)} + \frac{1}{1 - f_{NC}} \right\} \quad (A20)$$

Supplemental Table S1 can be used for easy calculating flux balance in any cells and in any circumstances provided that conditions specified by the model are observed.

Symbols and definitions

<i>Intracellular water and ion content</i>	
Water	Cell water (determined in present study by buoyant density) (ml (g protein) ⁻¹)
Na _i ⁺	Na ⁺ content (determined in present study by flame photometry) (μmol (g protein) ⁻¹)
K _i ⁺	K ⁺ content (determined in present study by flame photometry) (μmol (g protein) ⁻¹)
Cl ⁻	Cl ⁻ content (determined in present study by the steady-state ³⁶ Cl ⁻ distribution, specific radioactivity of the extracellular medium and [Cl] _o) (μmol (g protein) ⁻¹)
A	'Impermeant' osmolytes in cell (μmol (g protein) ⁻¹) A = ([Na] _o + [K] _o + [Cl] _o) × Water - (Na _i ⁺ + K _i ⁺ + Cl _i ⁻).
<i>Concentration of ions (mM)</i>	
[Na] _i , [K] _i , [Cl] _i	Concentration of ions in cell water
[Rb] _i	Intracellular Rb ⁺ concentration under the balanced state, [Rb] _i = [K] _i [Rb] _o /[K] _o
[Na] _o , [K] _o , [Cl] _o , [Rb] _o	Concentration of ions in extracellular medium
<i>Potentials</i>	
u	Membrane potential (dimensionless) (eqn (A11))
U	Membrane potential $U = uRT/F$; for 37°C $U = 26.7u$ (mV)
U ₀	Membrane potential when NKCC is absent (mV) (eqn (A12))
φ _K	'Equilibrium' potential for K ⁺ (Rb ⁺), $\varphi_K = \ln([K]o/[K]i)$ (dimensionless)
φ _{Cl}	'Equilibrium' potential for Cl ⁻ , $\varphi_{Cl} = \ln([Cl]i/[Cl]o)$ (dimensionless)
<i>Kinetic coefficients of ion Cl⁻ exchange and integral channel permeability</i>	
k	Rate constant of the total Cl ⁻ exchange (determined by ³⁶ Cl ⁻) (min ⁻¹)
P _{Na} , P _K , P _{Cl}	Coefficient of integral channel permeability of membrane for Na ⁺ , K ⁺ and Cl ⁻ (ml min ⁻¹ (g protein) ⁻¹) (eqns (A15)–(A17))
<i>Fluxes (μmol min⁻¹ (g protein)⁻¹)</i>	
I _{Cl} ^T	Total Cl ⁻ influx ≡ efflux determined by the kinetic of ³⁶ Cl ⁻ uptake or release under the balanced distribution of Cl ⁻ , $I_{Cl}^T = k \cdot Cl_i^-$
I _{Cl/Cl}	Flux related to the one-for-one Cl ⁻ exchanger
I _{Cl} ^t	Difference between the measured Cl ⁻ flux and the flux related to the one-for-one Cl ⁻ exchanger, $I_{Cl}^t = I_{Cl}^T - I_{Cl/Cl}$
I _{Cl} ^G	Cl ⁻ influx through electroconductive Cl ⁻ channels (eqn (A13))
J _{Cl} ^G	Cl ⁻ efflux through electroconductive Cl ⁻ channels (eqn (A14))
I _{Cl} ^{NKCC}	Cl ⁻ influx via NKCC pathway (eqn (A6))
J _{Cl} ^{NKCC}	Cl ⁻ efflux via NKCC pathway, $J_{Cl}^{NKCC} = -f_{NKCC} I_{Cl}^{NKCC}$
I _{Na} ^{NKCC}	Half the Cl ⁻ influx and the whole Na ⁺ or K ⁺ influxes via NKCC pathway
J _{Na} ^{NKCC}	Half the Cl ⁻ efflux and the whole Na ⁺ or K ⁺ effluxes via NKCC pathway, $J_{Na}^{NKCC} = -f_{NKCC} I_{Na}^{NKCC}$
I _{Cl} ^{NC}	Influx Na ⁺ and Cl ⁻ via NC cotransport $I_{Na}^{NC} = I_{Cl}^{NC}$, calculated by eqn (A4)
J _{Cl} ^{NC}	Efflux of Na ⁺ and Cl ⁻ via NC cotransport, $J_{Cl}^{NC} = -f_{NC} I_{Cl}^{NC}$
J _{Na} ^P	'Pump' Na ⁺ efflux, $J_{Na}^P = -(3/2)I_K^P$
I _K ^P	'Pump' K ⁺ influx
I _{Rb} ^T	Total Rb ⁺ influx estimated by Rb ⁺ flame photometry
I _{Rb} ^{OR}	Ouabain-resistant Rb ⁺ influx in the presence of ouabain
I _{Rb} ^P	Ouabain sensitive, the 'pump' Rb ⁺ influx, $I_{Rb}^P = I_{Rb}^T - I_{Rb}^{OR}$
I _{Rb} ^G	Rb ⁺ influx through channels
J _{Rb} ^G	Rb ⁺ efflux through channels
f _{NKCC} , f _{NC}	Ratio between efflux and influx via cotransporters NKCC or, respectively, NC (eqns (A2.1) and (A2.2))

References

- Arrebola F, Cañizares J, Cubero MA, Crespo PV, Warley A & Fernández-Segura E (2005a). Biphasic behavior of changes in elemental composition during staurosporine-induced apoptosis. *Apoptosis* **10**, 1317–1331.
- Arrebola F, Zabiti S, Cañizares FJ, Cubero MA, Crespo PV & Fernández-Segura E (2005b). Changes in intracellular sodium, chlorine, and potassium concentrations in staurosporine-induced apoptosis. *J Cell Physiol* **204**, 500–507.
- Arrebola F, Fernández-Segura E, Campos A, Crespo PV, Skepper JN & Warley A (2006). Changes in intracellular electrolyte concentrations during apoptosis induced by UV irradiation of human myeloblastic cells. *Am J Physiol Cell Physiol* **290**, C638–C649.
- Aull F, Nachbar MS & Oppenheim JD (1977). Chloride self exchange in Ehrlich ascites cells. *Biochim Biophys Acta* **471**, 341–347.
- Bortner CD & Cidlowski JA (2007). Cell shrinkage and monovalent cation fluxes: role in apoptosis. *Arch Biochem Biophys* **462**, 176–188.
- Bortner CD, Gomez-Angelats M & Cidlowski JA (2001). Plasma membrane depolarization without repolarization is an early molecular event in anti-Fas-induced apoptosis. *J Biol Chem* **276**, 4304–4314.
- Burg ED, Remillard CV & Yuan JX (2006). K^+ channels in apoptosis. *J Membr Biol* **209**, 3–20.
- D'Anglemon de Tassigny A, Souktani R, Henry P, Ghaleh B & Berdeaux A (2004). Volume-sensitive chloride channels ($I_{Cl,vol}$) mediate doxorubicin-induced apoptosis through apoptotic volume decrease in cardiomyocytes. *Fundam Clin Pharmacol* **18**, 531–538.
- Drummond GB (2006). Reporting ethical matters in *The Journal of Physiology*: standards and advice. *J Physiol* **587**, 713–719.
- Fernández-Segura E, Cañizares FJ, Cubero MA, Warley A & Campos A (1999). Changes in elemental content during apoptotic cell death studied by electron probe X-ray microanalysis. *Exp Cell Res* **253**, 454–462.
- Franco R, Bortner CD & Cidlowski JA (2006). Potential roles of electrogenic ion transport and plasma membrane depolarization in apoptosis. *J Membr Biol* **209**, 43–58.
- Gamba G (2005). Molecular physiology and pathophysiology of electroneutral cation-chloride cotransporters. *Physiol Rev* **85**, 423–493.
- García-Soto JJ & Grinstein S (1990). Determination of the transmembrane distribution of chloride in rat lymphocytes: role of Cl^- - HCO_3^- exchange. *Am J Physiol Cell Physiol* **258**, C1108–C1116.
- Goldman D (1943). Potential, impedance and rectification in membranes. *J Gen Physiol* **27**, 37–60.
- Hoffmann EK (1982). Anion exchange and anion-cation co-transport systems in mammalian cells. *Philos Trans R Soc Lond B* **299**, 519–535.
- Hoffmann EK (1987). Volume regulation in cultured cells. In *Cell Volume Control: Fundamental and Comparative Aspects in Animal Cells*, ed. Kleinzeller A, pp. 125–180. Academic Press, New York.
- Hoffmann EK (2001). The pump and leak steady-state concept with a variety of regulated leak pathways. *J Membr Biol* **184**, 321–330.
- Hoffmann EK, Lambert IH & Pedersen SF (2009). Physiology of cell volume regulation in vertebrates. *Physiol Rev* **89**, 193–277.
- Hoffmann EK, Simonsen LO & Sjöholm C (1979). Membrane potential, chloride exchange, and chloride conductance in Ehrlich mouse ascites tumour cells. *J Physiol* **296**, 61–84.
- Ise T, Shimizu T, Lee EL, Inoue H, Kohno K & Okada Y (2005). Roles of volume-sensitive Cl^- channel in cisplatin-induced apoptosis in human epidermoid cancer cells. *J Membr Biol* **205**, 139–145.
- Jakobsson E (1980). Interactions of cell volume, membrane potential, and membrane transport parameters. *Am J Physiol Cell Physiol* **238**, C196–C206.
- Kerr JF (1971). Shrinkage necrosis: a distinct mode of cellular death. *J Pathol* **105**, 13–20.
- Ladoux A, Krawice I, Cragoe EJ, Abita JP & Frelin C (1987). Properties of the Na^+ -dependent Cl^-/HCO_3^- exchange system in U937 human leukemic cells. *Eur J Biochem* **170**, 43–49.
- Lambert IH, Hoffmann EK & Jorgensen F (1989). Membrane potential, anion and cation conductances in Ehrlich ascites tumour cells. *J Membr Biol* **111**, 113–131.
- Lambert IH, Hoffmann EK & Pedersen SF (2008). Cell volume regulation: physiology and pathophysiology. *Acta Physiol* **194**, 255–282.
- Lang F, Föller M, Lang K, Lang P, Ritter M, Vereninov A, Szabo I, Huber SM & Gulbins E (2007). Cell volume regulatory ion channels in cell proliferation and cell death. *Methods Enzymol* **428**, 209–225.
- Lang F, Gulbins E, Szabo I, Vereninov A & Huber SM (2008). Ion channels, cell volume, cell proliferation and apoptotic cell death. In *Sensing with Ion Channels*, ed. Martinac B, pp. 69–84. Springer Verlag, Berlin, Heidelberg.
- Lang F, Shumilina E, Ritter M, Gulbins E, Vereninov A & Huber SM (2006). Ion channels and cell volume in regulation of cell proliferation and apoptotic cell death. *Contrib Nephrol* **152**, 142–160.
- Levinson C (1985). Sodium-dependent ion cotransport in steady state Ehrlich ascites tumor cells. *J Membr Biol* **87**, 121–130.
- Lew VL & Bookchin RM (1986). Volume, pH, and ion-content regulation in human red cells: analysis of transient behavior with an integrated model. *J Membr Biol* **92**, 57–74.
- Maeno E, Ishizaki Y, Kanaseki T, Hazama A & Okada Y (2000). Normotonic cell shrinkage because of disordered volume regulation is an early prerequisite to apoptosis. *Proc Natl Acad Sci U S A* **97**, 9487–9492.
- Maeno E, Shimizu T & Okada Y (2006). Normotonic cell shrinkage induces apoptosis under extracellular low Cl^- conditions in human lymphoid and epithelial cells. *Acta Physiol* **187**, 217–222.
- Nobel CS, Aronson JK, Van Den Dobbelen DJ & Slater AF (2000). Inhibition of Na^+/K^+ -ATPase may be one mechanism contributing to potassium efflux and cell shrinkage in CD95-induced apoptosis. *Apoptosis* **5**, 153–163.

- Okada Y & Maeno E (2001). Apoptosis, cell volume regulation and volume-regulatory chloride channels. *Comp Biochem Physiol A Mol Integr Physiol* **130**, 377–383.
- Okada Y, Sato K & Numata T (2009). Pathophysiology and puzzles of the volume-sensitive outwardly rectifying anion channel. *J Physiol* **587**, 2141–2149.
- Okada Y, Shimizu T, Maeno E, Tanabe S, Wang X & Takahashi N (2006). Volume-sensitive chloride channels involved in apoptotic volume decrease and cell death. *J Membr Biol* **209**, 21–29.
- Ouadid-Ahidouch H, Roudbaraki M, Delcourt P, Ahidouch A, Joury N & Prevarskaya N (2004). Functional and molecular identification of intermediate-conductance Ca²⁺-activated K⁺ channels in breast cancer cells: association with cell cycle progression. *Am J Physiol Cell Physiol* **287**, C125–C134.
- Poulsen, KA, Andersen ES, Hansen CF, Klausen TK, Hougaard C, Lambert IH & Hoffmann EK (2010). Deregulation of apoptotic volume decrease and ionic movements in multidrug-resistant tumor cells: role of chloride channels. *Am J Physiol Cell Physiol* **298**, C14–C25.
- Rubashkin AA, Yurinskaya VE & Vereninov AA (2010). Calculations of K⁺, Na⁺ and Cl⁻ fluxes across cell membrane with Na⁺/K⁺ pump, NKCC, NC cotransport and ionic channels with non-Goldman rectification in K⁺ channels: normal and apoptotic cells (in Russian). *Tsitologiya* **52**, 568–573. (in English: *Cell and Tissue Biol.* **4**, 464–470).
- Russell JM (2000). Sodium-potassium-chloride cotransport. *Physiol Rev* **80**, 211–276.
- Simchowicz L & De Weer P (1986). Chloride movements in human neutrophils diffusion, exchange, and active transport. *J Gen Physiol* **88**, 167–194.
- Simchowicz L, Ratzlaff R & De Weer P (1986). Anion/anion exchange in human neutrophils. *J Gen Physiol* **88**, 195–217.
- Skepper JN, Karydis I, Garnett MR, Hegyi L, Hardwick SJ, Warley A, Mitchinson MJ & Cary NR (1999). Changes in elemental concentrations are associated with early stages of apoptosis in human monocyte-macrophages exposed to oxidized low-density lipoprotein: an X-ray microanalytical study. *J Pathol* **188**, 100–106.
- Ussing HH (1949). The distinction by means of tracers between active transport and diffusion. *Acta Physiol Scand* **19**, 43–56.
- Vereninov AA, Goryachaya TS, Moshkov AV, Vassilieva IO, Yurinskaya VE, Lang F & Rubashkin AA (2007). Analysis of the monovalent ion fluxes in U937 cells under the balanced ion distribution: recognition of ion transporters responsible for changes in cell ion and water balance during apoptosis. *Cell Biol Int* **31**, 382–393.
- Vereninov AA, Rubashkin AA, Goryachaya TS, Moshkov AV, Rozanov YM, Shirokova AV, Strelkova EG, Lang F & Yurinskaya VE (2008). Pump and channel K (Rb⁺) fluxes in apoptosis of human lymphoid cell line U937. *Cell Physiol Biochem* **22**, 187–194.
- Vereninov AA, Yurinskaya VE & Rubashkin AA (2004). The role of potassium, potassium channels, and symporters in the apoptotic cell volume decrease: experiment and theory. *Dokl Biol Sci* **398**, 417–420.
- Vereninov AA, Yurinskaya VE & Rubashkin AA (2006). Apoptotic shrinkage of lymphoid cells: a model of changes in ion flux balance. *Dokl Biochem Biophys* **411**, 356–360.
- Wonderlin WF, Woodfork KA & Strobl JS (1995). Changes in membrane potential during the progression of MCF-7 human mammary tumor cells through the cell cycle. *J Cell Physiol* **165**, 177–185.
- Yurinskaya V, Goryachaya T, Guzhova I, Moshkov A, Rozanov Y, Sakuta G, Shirokova A, Shumilina E, Vassilieva I, Lang F & Vereninov A (2005a). Potassium and sodium balance in U937 cells during apoptosis with and without cell shrinkage. *Cell Physiol Biochem* **16**, 155–162.
- Yurinskaya VE, Goryachaya TS, Rubashkin AA, Shirokova AV & Vereninov AA (2010). Changes in K⁺, Na⁺, Cl⁻ balance and K⁺, Cl⁻ fluxes in U937 cells induced to apoptosis by staurosporine: on cell dehydration in apoptosis (in Russian). *Tsitologiya* **52**, 562–567. (in English: *Cell and Tissue Biol.* **4**, 457–463).
- Yurinskaya VE, Moshkov AV, Rozanov YM, Shirokova AV, Vassilieva IO, Shumilina EV, Lang F, Volgareva EV & Vereninov AA (2005b). Thymocyte K⁺, Na⁺ and water balance during dexamethasone- and etoposide-induced apoptosis. *Cell Physiol Biochem* **16**, 15–22.

Author contributions

All authors contributed equally to this work and all approved the final version.

Acknowledgements

We are grateful to Professor Florian Lang for thoughtful discussions and to Professor Andrey E. Vassilyev for valuable advice. This study was supported by the Russian Foundation for Basic Research, projects no. 09-04-00301a and by the Deutsche Forschungsgemeinschaft (436 RUS 113/488/0-2R, RFBR 06-04-04000).